3

Effect of Pulse Laser Duration and Shape on PLD Thin Films Morphology and Structure

Carmen Ristoscu and Ion N. Mihailescu
National Institute for Lasers, Plasma and Radiation Physics,
Lasers Department, Magurele, Ilfov
Romania

1. Introduction

Lasers are unique energy sources characterized by spectral purity, spatial and temporal coherence, which ensure the highest incident intensity on the surface of any kind of sample. Each of these characteristics stays at the origin of different applications. The study of high-intensity laser sources interaction with solid materials was started at the beginning of laser era, i.e. more than 50 years ago. This interaction was called during time as: vaporization, pulverization, desorption, etching or laser ablation (Cheung 1994). Ablation was used for the first time in connection with lasers for induction of material expulsion by infrared (IR) lasers. The primary interaction between IR photons and material takes place by transitions between vibration levels.

The plasma generated and supported under the action of high-intensity laser radiation was for long considered as a loss channel only and therefore, a strong hampering in the development of efficient laser processing of materials. In time, it was shown that the plasma controls not only the complex interaction phenomena between the laser radiation and various media, but can be used for improving laser radiation coupling and ultimately the efficient processing of materials (Mihailescu and Hermann, 2010).

The plasma generated under the action of fs laser pulses was investigated by optical emission spectroscopy (OES) and time-of-flight mass spectrometry (TOF-MS) (Ristoscu et al., 2003; Qian et al., 1999; Pronko et al., 2003; Claeyssens et al., 2002; Grojo et al., 2005; Amoruso et al., 2005a).

Lasers with ultrashort pulses have found in last years applications in precise machining, laser induced spectroscopy or biological characterization (Dausinger et al., 2004), but also for synthesis and/or transfer of a large class of materials: diamond-like carbon (DLC) (Qian et al., 1999; Banks et al., 1999; Garrelie et al., 2003), oxides (Okoshi et al., 2000; Perriere et al., 2002; Millon et al., 2002), nitrides (Zhang et al., 2000; Luculescu et al., 2002; Geretovszky et al., 2003; Ristoscu et al., 2004), carbides (Ghica et al., 2006), metals (Klini et al., 2008) or quasicrystals (Teghil et al., 2003). Femtosecond laser pulses stimulate the apparition of non-equilibrium states in the irradiated material, which lead to very fast changes and development of metastable phases. This way, the material to be ablated reaches the critical point which control the generation of nanoparticles (Eliezer et al., 2004; Amoruso et al., 2005b; Barcikowski et al., 2007; Amoruso et al., 2007).

Pulse shaping introduces the method that makes possible the production of tunable arbitrary shaped pulses. This technique has already been applied in femtochemistry (Judson and Rabitz, 1992), to the study of plasma plumes (Singha et al., 2008; Guillermin et al., 2009), controlling of two-photon photoemission (Golan et al., 2009), or coherent control experiments in the UV where many organic molecules have strong absorption bands (Parker et al., 2009). Double laser pulses were shown to be promising in laser-induced breakdown spectroscopy (Piñon et al., 2008), since they allow for the increase of both ion production and ion energy. The spatial pulse shaping is required to control the composition of the plume and to achieve the fully atomized gas phase by a single subpicosecond laser pulse (Gamaly et al., 2007).

Temporally shaping of ultrashort laser pulses by Fourier synthesis of the spectral components is an effective technique to control numerous physical and chemical processes (Assion et al., 1998), like: the control of ionization processes (Papastathopoulos et al., 2005), the improvement of high harmonic soft X-Rays emission efficiency (Bartels et al., 2000), materials processing (Stoian et al., 2003; Jegenyes et al., 2006; Ristoscu et al., 2006) and spectroscopic applications (Assion et al., 2003; Gunaratne et al., 2006).

The adaptive pulse shaping has been applied for ion ejection efficiency (Colombier et al, 2006; Dachraoui and Husinsky, 2006), generation of nanoparticles with tailored size (Hergenroder et al., 2006), applications in spectroscopy and pulse characterization (Ackermann et al., 2006; Lozovoy et al., 2008).

In materials science, pulsed laser action results in various applications such as localized melting, laser annealing, surface cleaning by desorption and ablation, surface hardening by rapid quench, and after 1988, pulsed laser deposition (PLD) technologies for synthesizing high quality nanostructured thin films (Miller 1994; Belouet 1996; Chrisey and Hubler, 1994; Von Allmen and Blatter, 1995). The laser – target interaction is a very complex physical phenomenon. Theoretical descriptions are multidisciplinary and involve equilibrium and non-equilibrium processes.

There are several consistent attempts in the literature for describing the interaction of ultrashort laser pulses with materials, especially metallic ones (Kaganov et al., 1957; Zhigilei and Garrison, 2000). Conversely, there are only a few that deal with the interaction of ultrashort pulses with wide band gap (dielectric, insulator and/or transparent) materials. Itina and Shcheblanov (Itina and Shcheblanov, 2010) recently proposed a model based on simplified rate equations instead of the Boltzmann equation to predict excitation by ultrashort laser pulses of conduction electrons in wide band gap materials, the next evolution of the surface reflectivity and the deposition rate. The analysis was extended from single to double and multipulse irradiation. They predicted that under optimum conditions the laser absorption can become smoother so that both excessive photothermal and photomechanical effects accompanying ultrashort laser interactions can be attenuated. On the other hand, temporally asymmetric pulses were shown to significantly affect the ionization process (Englert et al., 2007; Englert et al., 2008).

Implementation of PLD by using ps or sub-ps laser has been predicted to be more precise and expected to lead to a better morphology, in comparison to experiments performed with nanosecond laser pulses (Chichkov et al., 1996; Pronko et al., 1995). Clean ablation of solid targets is achieved without the evidence of the molten phase, due to the insignificant thermal conduction inside the irradiated material during the sub-ps and fs laser pulse action. Accordingly, ablation with sub-ps laser pulses was expected to produce much smoother film surfaces than those obtained by ns laser pulses (Miller and Haglund, 1998). It

was shown that many parameters have to be monitored in order to get thin films with the desired quality. They are, but not limited to: the laser intensity distribution, scanning speed of the laser focal spot across the target surface, energy of the pre-pulse (in case of Ti-sapphire lasers) or post-pulse (for excimer lasers), pressure and nature of the gas in the reaction chamber, and so on.
In this chapter we review results on the effect of pulse duration upon the characteristics of nanostructures synthesized by PLD with ns, sub-ps and fs laser pulses. The materials morphology and structure can be gradually modified when applying the shaping of the ultra-short fs laser pulses into two pulses succeeding to each other under the same temporal envelope as the initial laser pulse, or temporally shaped pulse trains with picosecond separation (mono-pulses of different duration or a sequence of two pulses of different intensities).

2. Role of laser pulse duration in deposition of AlN thin films

Aluminum nitride (AlN), a wide band gap semiconductor (Eg= 6.2 eV), is of interest for key applications in crucial technological sectors, from acoustic wave devices on Si, optical coatings for spacecraft components, electroluminescent devices in the wavelength range from 215 nm to the blue end of the optical spectrum, as well as heat sinks in electronic packaging applications, where films with suitable surface finishing (roughness) are requested. The effect of laser wavelength, pulse duration, and ambient gas pressure on the composition and morphology of the AlN films prepared by PLD was investigated (Ristoscu et al., 2004). We worked with three laser sources generating pulses of 34 ns@248 nm (source A), 450 fs@248 nm (source B), and 50 fs@800 nm (source C). We have demonstrated that the duration of the laser pulse is an important parameter for the quality and performances of AlN structures.
Using PLD technique (Fig. 1), AlN thin films well oriented (Gyorgy et al., 2001) and having good piezoelectric properties can be obtained. The laser beam was focused onto the surface of a high purity (99.99%) AlN target, at an incidence angle of about 45° with respect to the target surface. The laser fluence incident onto the target surface was set at 0.1, 0.2 and 0.4 J/cm^2. For deposition of one film, we applied the laser pulses for 15 or 20 minutes.

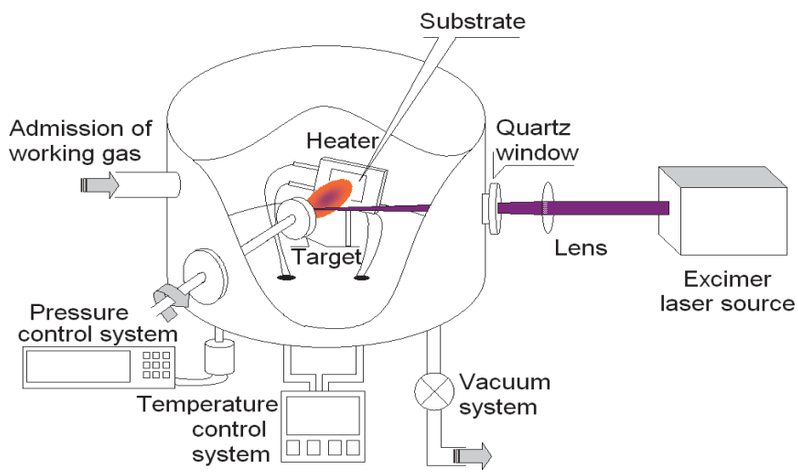

Fig. 1. PLD general setup used in the experiments reviewed in this chapter

Before each deposition the irradiation chamber was evacuated down to a residual pressure of ~ 10^{-6} Pa. The depositions have been conducted in vacuum (5x10^{-4} Pa) or in very low dynamic nitrogen pressure at values in the range (1-5)x10^{-1} Pa. During PLD deposition the substrates were heated up to 750 °C. The target-substrate separation distance was 4 cm. AlN thin films were deposited on various substrates: oxidized silicon wafers and oxidized silicon wafers covered with a platinum film, glass plates, suitable for various characterization techniques.
In the following, we will present detailed results for the PLD films deposited with source C. The synthesized structures were rather thin, having a thickness of 90-100 nm. The film deposited with the highest laser fluence (0.4 J/cm^2) has a thickness of about 400 nm.

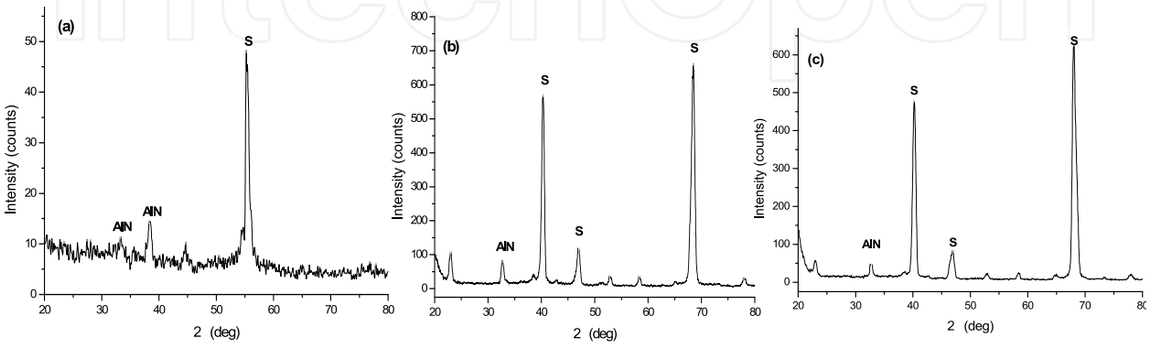

Fig. 2. XRD patterns of the films deposited from AlN target in vacuum (5x10^{-4} Pa) (a), 0.1 Pa N_2 (b), and 0.5 Pa N_2 (c), respectively (Cu Kα radiation); S stands for substrate

Typical XRD patterns recorded for PLD AlN films are given in Figs. 2a-c. For the films obtained in vacuum (Fig. 2a), 0.1 Pa N_2 (Fig. 2b) as well as 0.5 Pa N_2 (Fig. 2c), a low intensity peak is present in the XRD patterns. This peak placed at 33° is assigned to AlN <100> hexagonal phase. The low intensity is due to the fact that the films are rather thin. Along with this peak, some other lines assigned to the substrate are present. Anyhow, the peaks attributed to AlN are quite large. This is indicative in our opinion for a mixture of crystalline and amorphous phases in the deposited films. This mixture was formed as an effect of the depositions temperature, 750^o C. Previous depositions in which we evidenced only crystalline AlN were performed at 900^o C (Gyorgy et al., 2001).
SEM investigations of the films (Figs. 3a-c) showed that the number of the particulates observed on the surface decreases with the increase of the ambient gas pressure, but their dimensions increase. The particulates present on films surface have spherical shape, with diameters in the range (100-800) nm.

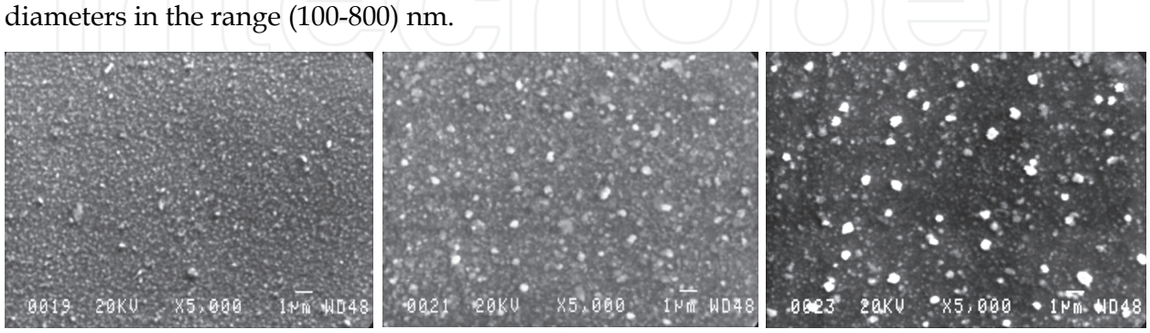

(a) (b) (c)

Fig. 3. SEM images of the films deposited from AlN target in vacuum (5x10^{-4} Pa) (a), 0.1 Pa N_2 (b), and 0.5 Pa N_2 (c), respectively

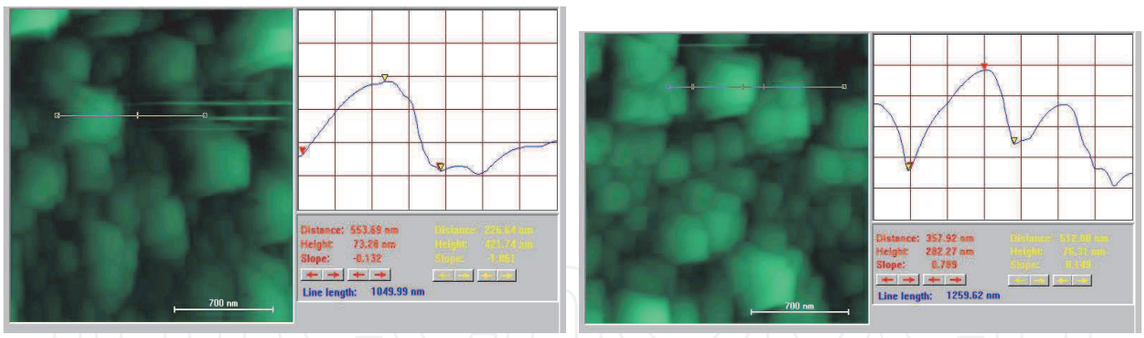

(a) (b)

Fig. 4. AFM pictures of AlN thin films obtained from AlN target in 0.1 Pa N_2 (a), and 0.5 Pa N_2 (b)

From AFM images (Figs. 4a,b), we observed that the size of grains reaches hundreds of nanometers, increasing from sample a) to sample b), in good agreement with thickness measurements and SEM investigations.

In Table 1 we summarized the characteristics of AlN thin films obtained with the three laser sources, along with the deposition rate.

Pressure	Laser wavelength	Frequency repetition rate	Pulse duration	Incident laser fluence	Phase content	Observations
Vacuum ($5x10^{-5}$ Pa)	248 nm	10 Hz	34 ns (A)	4 J / cm²	Al(111)c, Al(200)c, Al(220)c, AlN(002)h	Microcrystallites in dendrite arrangements, 0.7 Å/pulse
	248 nm	10 Hz	450 fs (B)	4 J / cm²	AlN(100)h	Droplets with diameters of 100 nm - 1µm, 0.05 Å/pulse
	800 nm	1 kHz	50 fs (C)	0.4J / cm²	AlN(100)h	Droplets of less 1 µm diameter, 0.0033 Å/pulse
0.5 Pa N_2	248 nm	10 Hz	34 ns (A)	4 J / cm²	AlN(100)h, AlN(002)h	1D low amplitude undulation 0.7 Å/pulse
	248 nm	10 Hz	450 fs (B)	4 J / cm²	AlN(100)h	Droplets of less 1 µm diameters, 0.01 Å/pulse
	800 nm	1 kHz	50 fs (C)	0.4 J / cm²	AlN(100)h	Lower droplets density than in vacuum, 0.0033 Å/pulse

Table 1. Main characteristics of AlN deposited films

We observed that only AlN was detected in the films obtained with laser sources B and C, while films obtained with source A contain a significant amount of metallic Al. The increase of N_2 pressure causes crystalline status perturbation for films deposited with sources B and C, but compensates N_2 loss when working with source A. The lowest density of particulates was observed for films obtained with source A. It dramatically increases (4-5 orders of magnitude) for sources B and C. The deposition rate exponentially decreases from sources A to C. These behaviors well corroborate with target examination. The crater on the surface of the target submitted to source A gets metallised in time, while the other two craters preserve the ceramic aspect. OES and TOF-MS investigations are in agreement with the studies of films, showing plasma richer in Al ions for source A (Ristoscu et al., 2003). Our studies evidenced the prevalent presence of AlN positive ions in the plasma generated under the action of sources B and C.
We deposited stoichiometric and even textured AlN thin films by PLD from AlN targets using a Ti-sapphire laser system generating pulses of 50 fs@800 nm (source C).

3. Temporal shaping of ultrashort laser pulses

Ref. (Stoian et al., 2002) demonstrated a significant improvement in the quality of ultrafast laser microstructuring of dielectrics when using temporally shaped pulse trains. Dielectric samples were irradiated with pulses from an 800 nm/1 kHz Ti:sapphire laser system delivering 90 fs pulses at 1.5 mJ. They used single sequences of identical, double and triple pulses of different separation times (0.3–1 ps) and equal fluences (Fig. 5). The use of shaped pulses enlarges the processing window allowing the application of higher fluences and number of sequences per site while keeping fracturing at a reduced level. For brittle materials with strong electron-phonon coupling, the heating control represents an advantage. The sequential energy delivery induced a material softening during the initial steps of excitation, changing the energy coupling for the subsequent steps. This leaded to cleaner structures with lower stress. Temporally shaped femtosecond laser pulses would thus allow exploitation of the dynamic processes and control thermal effects to improve structuring.

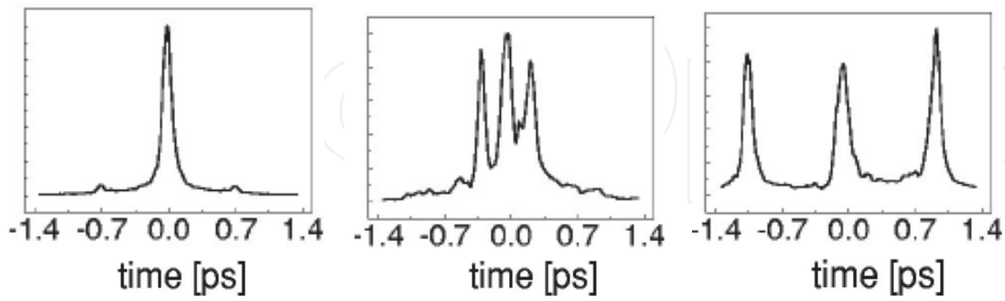

Fig. 5. Single pulses and triple-pulse sequences with different separation times (0.3–1 ps) and equal fluences (Stoian et al., 2002)

Ref. (Guillermin et al., 2009) reports on the possibility of tailoring the plasma plume by adaptive temporal shaping. The outcome has potential interest for thin films elaboration or nanoparticles synthesis. A Ti:saphirre laser beam (centered at 800 nm) with 150 fs pulse duration was used in their experiments. The pulses from the femtosecond oscillator are

spectrally dispersed in a zero-dispersion unit and the spatially-separated frequency components pass through a pixellated liquid crystal array acting as a Spatial Light Modulator (SLM). The device allows relative retardation of spectral components, tailoring in turn the temporal shape of the pulse. They applied an adaptive optimization loop to lock up temporal shapes fulfilling user-designed constraints on plasma optical emission. The pulses with a temporal form expanding on several ps improved the ionic vs. neutral emission and allowed an enhancement of the global emission of the plasma plume.
Temporally shaped femtosecond laser pulses have been used for controlling the size and the morphology of micron-sized metallic structures obtained by using the Laser Induced Forward Transfer (LIFT) technique. Ref. (Klini et al., 2008) presents the effect of pulse shaping on the size and morphology of the deposited structures of Au, Zn, Cr. The double pulses of variable intensities with separation time Δt (from 0 to 10 ps) were generated by using a liquid crystal SLM (Fig. 6).

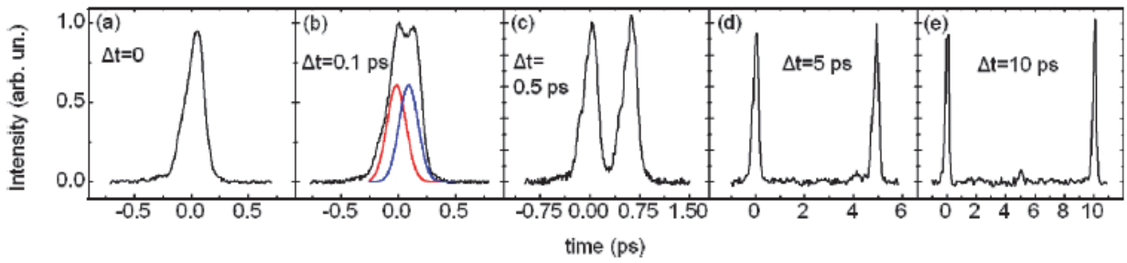

Fig. 6. Temporal pulse profiles generated with the method described in the text. Red and blue profiles in (b) are a guide to the eye to represent the underlying double pulses (Klini et al., 2008)

The laser source used for the pump-probe experiments was a Ti:Sapphire oscillator delivering 100 fs long pulses at 800 nm and with a 80 MHz repetition rate.
The temporal shape of the excitation pulse and the time scales of the ultrafast early stage processes occurring in the material can influence the morphology and the size of the LIFT dots. For Cr and Zn the electron-phonon coupling is relatively strong, and the morphology of the transferred films is determined by the electron-phonon scattering rate, i.e. very fast and within the pulse duration for Cr, and in the few picoseconds time scale for Zn. For Au the electron-phonon coupling is weak but the fast ballistic transport of electrons is very efficient. The numerous collisions of electrons with the film's surfaces determine the morphology. The internal electron thermalization rate which controls the electron-lattice coupling strength may determine the films' sizes.
The observed differences in size and morphology are correlated with the conclusion of pump-probe experiments for the study of electron-phonon scattering dynamics and subsequent energy transfer processes to the bulk. (Klini et al., 2008) proposed that in metals with weak electron-lattice coupling, the electron ballistic motion and the resulting fast electron scattering at the film surface, as well as the internal electron thermalization process are crucial to the morphology and size of the transferred material. Therefore, temporal shaping within the corresponding time scales of these processes may be used for tailoring the features of the metallic structures obtained by LIFT.
We mention here other approaches to obtain shaped pulses. Refs. (Hu et al., 2007) and (Singha et al., 2008) used an amplified Ti:sapphire laser (Spectra Physics Tsunami oscillator

and Spitfire amplifier), which delivers 800 nm, 45 fs pulses with a maximum pulse energy of 2 mJ at a 1 kHz repetition rate and a Michelson interferometer to generate double pulses with a controllable delay of up to 110 ps. An autocorrelation measurement showed that the pulse is stretched by the subsequent optics to 80 fs. Ref. (Golan et al., 2009) introduced the output from the frequency doubled mode-locked Ti-sapphire laser (60 fs pulses at 430 nm, having energy of about 0.4 nJ per pulse) into a programmable pulse shaper composed of a pair of diffraction gratings and a pair of cylindrical lenses. A pair of one-dimensional programmable liquid-crystal SLM arrays is placed at the Fourier plane of the shaper. These arrays are used as a dynamic filter for spectral phase manipulation of the pulses. Using a pair of SLM arrays provides an additional degree of freedom and therefore allows some control over the polarization of the pulse. Ref. (Parker et al., 2009) uses a reflective mode, folded, pulse shaping assembly employing SLM shapes femtosecond pulses in the visible region of the spectrum. The shaped visible light pulses are frequency doubled to generate phase- and amplitude-shaped, ultra-short light pulses in the deep ultraviolet.

4. Temporally shaped vs. unshaped ultrashort laser pulses applied in PLD of SiC

Semiconductor electronic devices and circuits based on silicon carbide (SiC) were developed for the use in high-temperature, high-power, and/or high-radiation conditions under which devices made from conventional semiconductors cannot adequately perform. The ability of SiC-based devices to function under such extreme conditions is expected to enable significant improvements in a variety of applications and systems. These include greatly improved high-voltage switching for saving energy in electric power distribution and electric motor drives, more powerful microwave electronic circuits for radar and communications, sensors and controllers for cleaner burning, more fuel-efficient jet aircraft and automobile engines (http://www.nasatech.com/Briefs/Feb04/LEW17186.html).

The excellent physical and electrical properties of silicon carbide, such as wide band gap (between 2.2 and 3.3 eV), high thermal conductivity (three times larger than that of Si), high breakdown electric field, high saturated electron drift velocity and resistance to chemical attack, defines it as a promising material for high-temperature, high-power and high-frequency electronic devices (Muller et al., 1994; Brown et al., 1996), as well as for opto-electronic applications (Palmour et al., 1993; Sheng et al., 1997).

In Ref. (Ristoscu et al., 2006) it was tested eventual effects of interactions of the time shaping of the ultra-short fs laser pulses into two pulses succeeding to each other under the same temporal envelope as the initial laser pulse. This proposal was different from that used in Ref. (Gamaly et al., 2004) in case of spatial pulse shaping. The spatial Gaussian shape of the laser pulses was preserved. As known (Gyorgy et al., 2004) and demonstrated in the section 2 of this chapter, high intensity fs laser ablation deposition produces mainly amorphous structures with a prevalent content of nanoparticulates. This seems to be the consequence of coupling features of ‘‘normal’’ fs laser pulses to solid targets. We tried to test the effect of detaching from the ‘‘main’’ pulse a first signal with intensity in excess of plasma ignition threshold (Fig. 7).

The ablation is then initiated by the first pre-pulse and the expulsed material is further heated under the action of the second, longer and more energetic pulse. One expects that by proper choice of temporal delay, the second pulse intercepts and overheats the particulates generated by the pre-pulse causing their gradual boiling and elimination. Ultimately, the

deposition of a film becomes possible with a lower particulates density (till complete elimination) and with a highly improved crystalline status.

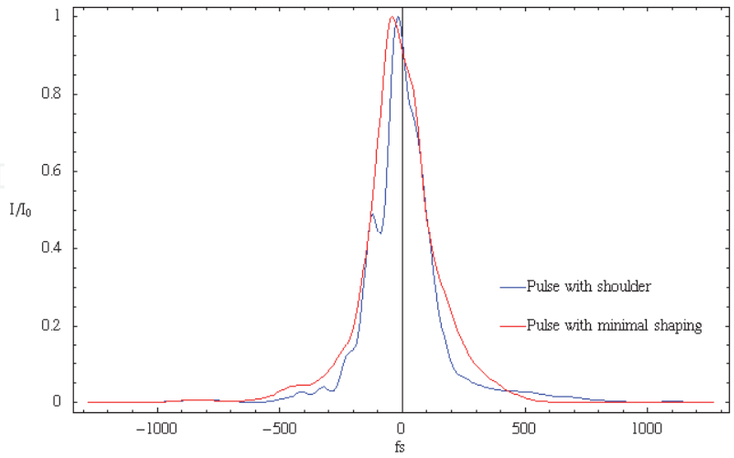

Fig. 7. Comparison between pulse shaped (blue) and plain amplifier (red)

The deposition experiments were conducted by PLD from bulk SiC target in vacuum (10^{-4} Pa), at temperatures around 750° C. The laser system was a Spectra Physics Tsunami with a BM Industries amplifier system giving 200 fs pulse duration with 600 mJ at 1 kHz and 800 nm wavelength, Fastlite Dazzler AOM system with controller and software driver running under LabView. The DAZZLER system is an acousto–optic programmable dispersive filter. It enables the separate control of both the spectral amplitude and the spectral phase. The crystal is an active optic component which, through the acousto–optic interaction, allows the spectral phase and amplitude shaping of an optical pulse. The general layout can be seen in Ref. (Verluise et al., 2000). We selected a generation regime where a pulse with a typical shape such as that shown in Fig. 7. The pulses were temporally characterized using the standard frequency-resolved optical gating (FROG) technique (Trebino and Kane, 1993; Trebino et al., 1997; DeLong et al., 1994). It enables both the phase and the amplitude of the pulse be retrieved simultaneously. More precisely, we applied the second harmonic generation (SHG) version of this technique using a thin BBO crystal as the NLO medium.

After optimization, we have chosen the following laser parameters: laser beam focused in spots of 0.07 mm^2, corresponding to a laser fluence on the target surface of 714 mJ/cm^2. For the deposition of one film we applied trains of subsequent laser pulses with a total duration of 15 min.

The SiC films obtained with unmodulated laser pulses are not fully crystallized, consisting in a nanostructured matrix incorporating well defined crystalline grains with elongated shapes (Ghica et al., 2006). A high density of {111} planar defects has been observed inside the crystalline grains, most probably formed by the dissociation of screw dislocations into partials on the {111} slip planes (Fig. 8). The dissociation of the screw dislocations and the motion of the partial dislocations on the slip planes may be triggered by the stress between adjacent growing grains or exerted by the highly energetic nanometric particles (droplets) resulting from the interaction between the target and the extremely short laser pulses.

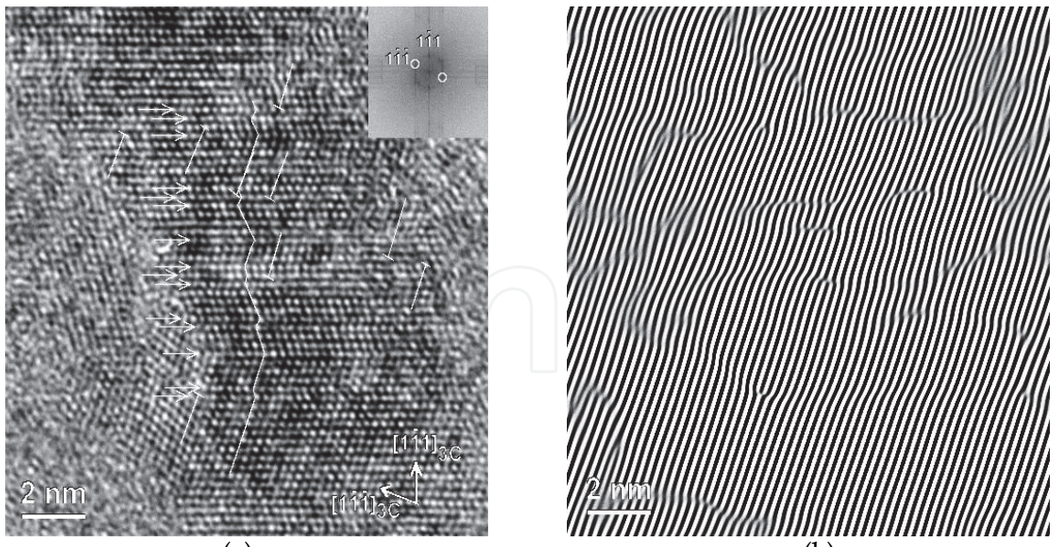

(a) (b)

Fig. 8. (a) HRTEM image along the (110)3C-SiC zone axis showing the bottom part of a SiC column; the trace of the (1-1-1) planes (the zig-zag line) and the position of the planar defects (arrows) are indicated; the Fourier transform (FFT) of the image is inserted in the upper right corner; (b) Bragg filtered image obtained by inverse FFT using the 1-1-1 and -111 pair of spots (encircled on the FFT image); the image contrast has been intentionally exaggerated in order to improve the visibility of the dislocations (Ghica et al., 2006)

In XRD patterns of the films deposited with tailored pulses, only the lines of Si (100) originating from the substrate and of β-SiC phase were visible. The formation of β-SiC was further supported by electron microscopy studies. Two important differences are to be emphasized with respect to samples deposited with unmodulated laser pulses:

i. The film surface is rather smooth, the roughness being dramatically reduced;
ii. The film is rather compact, showing no cracks, unlike the SiC films synthesized with unmodulated pulses, where a high density of fissures could be observed (Ghica et al., 2006). The cracks occurring are linked to the presence of droplets on the film surface and, further, to their high energy at the impact with the substrate. The lack of droplets or their low density leads to the growth of a compact film, free of cracks. This is precisely the case of thin structures deposited by tailored laser pulses.

For a comparison between the surface morphologies of the two types of films we give in Figs. 9a and c two characteristic SEM images. The fine structure of the surface of films obtained with unmodulated and tailored pulses is presented in the two SEM images recorded at higher magnification (Figs. 9b and d). The film synthesized with unmodulated laser pulses shows a high density of particulates (about 62 μm^{-2}), reaching up to 400 nm in size (Fig. 10a). Comparatively, a striking reduction of the droplets density can be observed for the film obtained with time tailored laser pulses, down to 8.6 μm^{-2} (Fig. 10b) The largest particulates also reach 400 nm.

We consider that this noticeable decrease of density along with the conservation of particulates dimension (in both size and distribution) is the effect of the particular pulse coupling mechanism which becomes effective in case of tailored laser pulses. The particulates generated by the first peak efficiently absorb the light in the second one, are vaporized and partially eliminated.

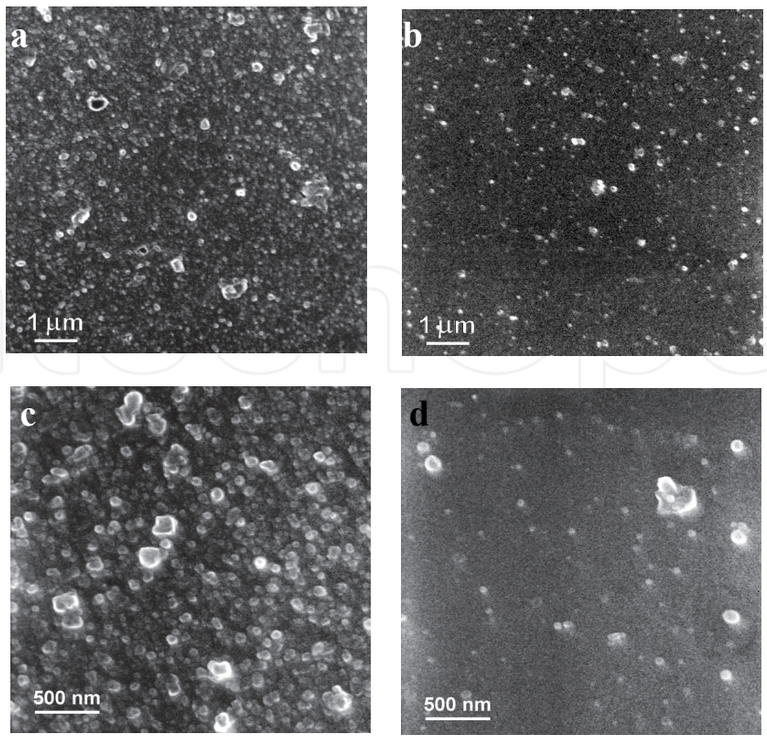

Fig. 9. SEM images showing the surface morphology of the samples obtained with unmodulated (a, c) and tailored (b, d) laser pulses (Ghica et al., 2006)

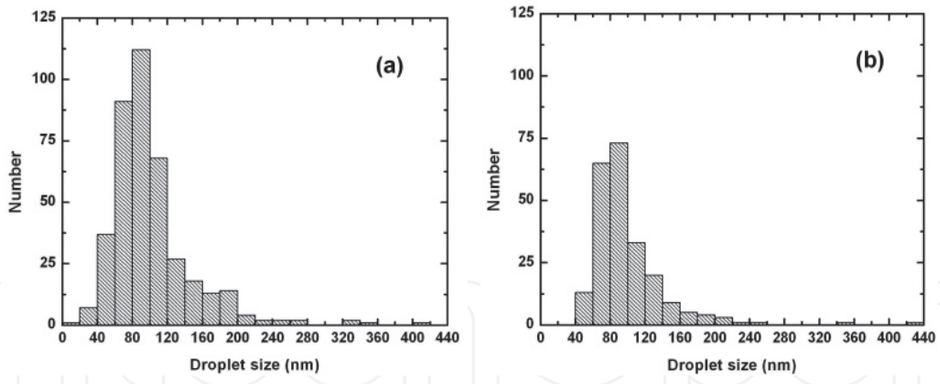

Fig. 10. Hystograms of the SiC samples obtained with unmodulated (a) and tailored (b) laser pulses

5. Temporally shaped ultrashort pulse trains applied in PLD of AlN

Amplified Ti:Sapphire laser pulses at 800 nm, 1 kHz repetition rate, with durations of 200 fs were used. The repetition rate was scaled down electronically to 1 Hz. Prior to amplification, a programmable liquid crystal SLM was inserted into the Fourier plane of a 4f zero-dispersion configuration (Weiner 2000), allowing temporal pulse shaping of the incoming beam to two pulses with the temporal separation determined by phase modulation. The phase mask for the generation of the pulse shapes was determined numerically using an

iterated Fourier transform method (Schmidt et al., n.d.). These generated shapes are then amplified thus compensating for spatio-temporal and energetic fluctuations that are inherent in this system (Wefers and Nelson, 1995; Tanabe et al., 2005). We selected a generation regime where the pulse has the typical shape shown in Fig. 11. The pulses were temporally characterized a standard frequency-resolved optical gating technique (Trebino 2002). This algorithm facilitates the simultaneous retrieve of both the phase and amplitude of the pulse. We applied the second harmonic generation (SHG) version of this technique using a thin BBO single crystal as the NLO medium where the ambiguity in the temporal symmetry of the retrieved pulses was resolved separately using an etalon.

We have chosen the following laser parameters: a laser beam spot of 0.08 mm^2 and an incident laser energy on the target surface of 400 μJ. For the deposition of one film we applied trains of laser pulses with a total duration of 20 min. The deposition of AlN thin films has been carried out in vacuum (10^{-4} Pa) at 800° C substrate temperature. Three types of samples have been deposited under identical conditions, with the exception of the shape of the laser pulse: AlN-1 with unshaped laser pulses, AlN-2 and AlN-3 using the shapes 2 and 3 respectively, given in Fig. 11.

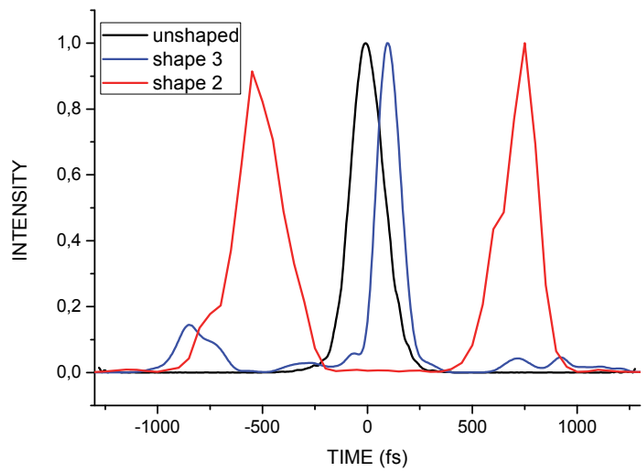

Fig. 11. Comparison between pulse shaped (blue, red) and plain amplifier (black)

For samples AlN-1 (Fig. 12a), we could identify three classes of surface particulates: particulates smaller than 100 nm, medium sized particulates up to 1 μm and large particulates, up to 2 μm. The large particulates were rather rare. The typical surfaces of the AlN-2 film (Fig. 12b) also showed large crystallites ranging up to 1.5 μm, with a rather high density. In the case of the AlN-3 samples (Fig. 12c), the particulates could be grouped in three classes on their average size: particulates around 100 nm, particulates around 500 nm and particulates larger than 1.5 μm up to 2.5 μm. The large particulates showed well defined facets.

The measured average particulates density was quite similar in the three cases, specifically $(5\pm0.8)x10^8$ cm^{-2} for the AlN-1 samples, $(4.8\pm0.7)x10^8$ cm^{-2} for the AlN-2 and $(5.6\pm0.8)x10^8$ cm^{-2} for the AlN-3 samples, with about 15% counting error in each case. Histograms of the microparticle size distribution in the case of the 3 types of samples were presented next to the corresponding SEM image. The particulates average size resulting from the histogram analysis was 390±5 nm in case of samples AlN-1, 230±3 nm for AlN-2 and 310±4 nm in case of samples AlN-3.

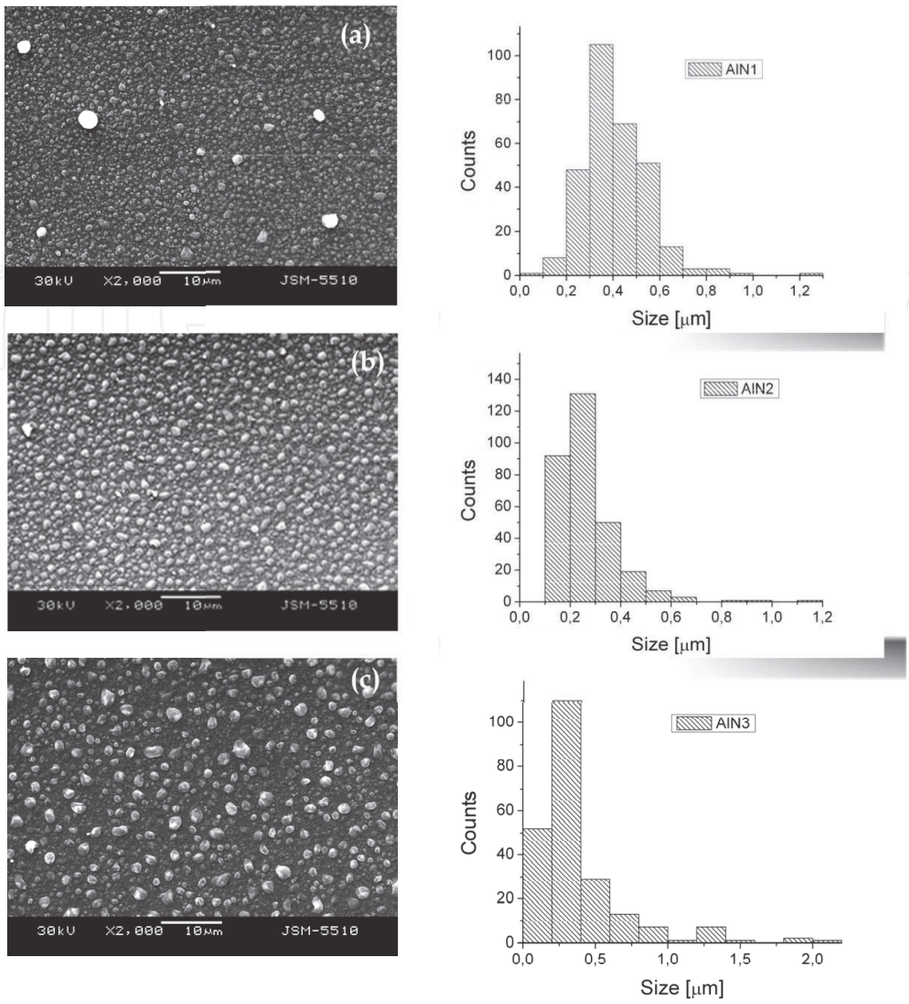

Fig. 12. SEM images showing the surface morphology of samples AlN-1 (a), AlN-2 (b) and AlN-3 (c) along with their histograms

From Fig. 11 we observed that the two pulses composing shapes 2 and 3 are separated at 1.25 ps and less than 1 ps, respectively. According to Ref. (Itina and Shcheblanov, 2010), this means that in both cases, the second pulse interacts with the plasma produced by the first one. Moreover, the 2 pulses were more or less equal as duration and intensity for shape 2, while for shape 3 the intensity of the second pulse is largely surpassing the one of the first pulse. As an effect, the second pulse is more efficient for samples AlN-2 in breaking the particulates generated under the action of the first one. This is visible in Figs. 12b and c which show larger and slightly more numerous particulates for samples AlN-3. As known, wide band-gap materials normally present a rather limited density of conduction electrons. Under intense (ultrashort) laser irradiation, the generation of a high number of conduction electrons is initiated, strongly influencing the electron interactions, and eventually determining the structural modifications of the material.

TEM investigations showed that the films are a mixture of crystalline and amorphous components. It is demonstrated that in dielectrics electron thermalization requires hundreds of fs (Bulgakova et al., 2010). The free-electron gas transfers energy to the lattice by coupling

to the vibration bath, which results in heating and triggering of a whole range of phase transformation processes in the material, including melting, ablation via the different mechanisms such as phase explosion, fragmentation, and upon cooling solidification with formation of amorphous and/or polycrystalline phases.
The AlN films deposited under the action of temporally shaped or unshaped fs laser pulses consisted of a mixture of crystalline phases characterized by the prevalent presence of hexagonal AlN and existence of metallic Al traces. SEM and TEM investigations showed that when using shaped pulses the number of large crystal grains in the films was increasing. On the other hand, the average grains size decreased by about a half as an effect of shaping.

6. Temporally shaped ultrashort pulse trains applied in PLD of SiC, ZnO and Al

A reduction of number of particulates accompanied by an increase of their size was observed for SiC when applying mono-pulses of different duration or passing to a sequence of two pulses of different intensities (see Fig. 11). The SiC structures present a smoother surface as compared with the other films (Figs. 13a-c). The average dimension of particulates is 150 nm for samples obtained with unshaped pulses. When using shape 2 laser pulses, the average dimension of the particulates present on surface of SiC films is ~ 100 nm, with a higher density than the structure obtained with unshaped pulses. Large particulates of ~1 μm can be observed on the surface of the films obtained with the shape 3 pulse, with the lowest density. For this material, when using this shaped pulse (a small shoulder well separated from a higher one) we obtained better surfaces.

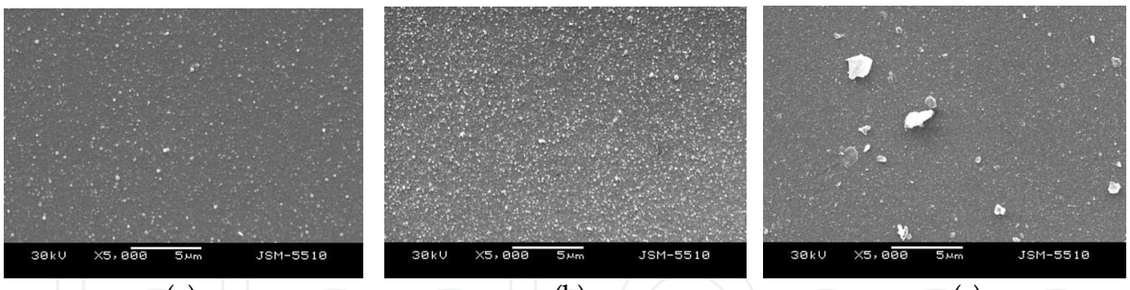

(a) (b) (c)

Fig. 13. SEM images showing the surface morphology of samples SiC when using unshaped (a), shape 2 (b) and shape 3 (c) laser pulses

Typical XRD pattern of the SiC films is presented in Fig. 14, wherefrom we can see only the line assigned to β-SiC phase.
On the other hand, in case of ZnO the best laser pulse which induces a dramatic decrease of particulate density was shape 2 (see Fig. 11). The deposition of ZnO thin films has been carried out in vacuum (10^{-4} Pa) at 350^{o} C substrate temperature. We generally obtained smooth surfaces with particulates lower than 100 nm (Figs. 15 a-c). The sample obtained with unshaped pulses exhibit a reduced roughness with fine particles having dimensions around 100 nm. The shape 2 laser pulses favored the development of a surface with large porosity and particulates of ~ 100 nm diameter. The shape 3 pulse induced also a porosity of the deposited film but a decrease of the particles size to ~ 50 nm.

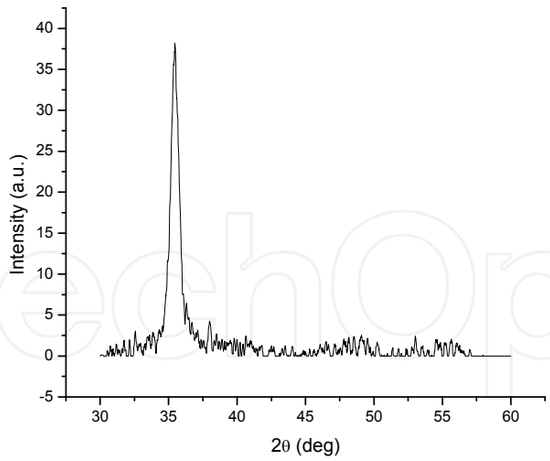

Fig. 14. Tipical XRD pattern of SiC film obtained with shape 3 laser pulses

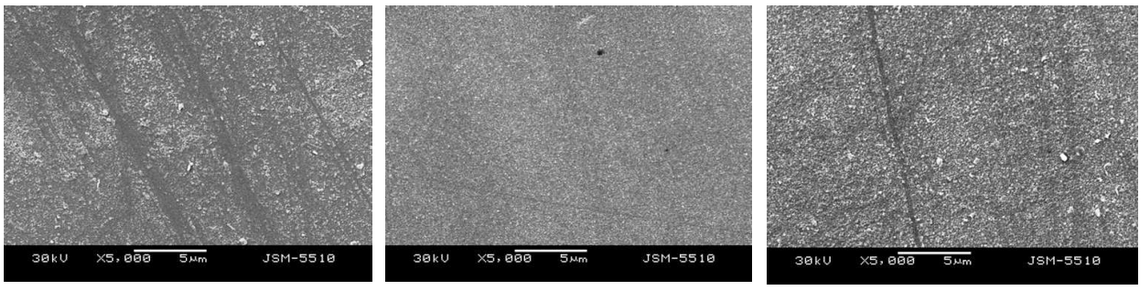

(a) (b) (c)

Fig. 15. SEM images showing the surface morphology of samples ZnO when using unshaped (a), shape 2 (b) and shape 3 (c) laser pulses

For ZnO samples we acquired also transmission spectra. The transmission was higher than 85% for all deposited structures, irrespective the shape of the ultra-short laser pulses.
In case of metallic targets, the obtained Al films present identical morphologies, irrespective of the pulse shape. Their surfaces are rough with micro-particles having an average dimension of about 1 μm (Figs. 16 a,b). Moreover, the microparticulates are well connected to each other, suggesting that they arrive on substrate in liquid phase.

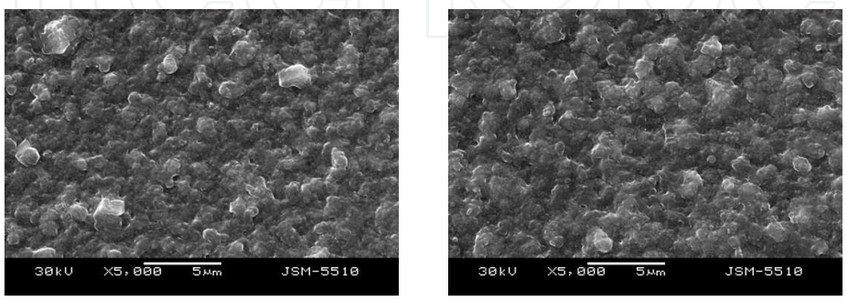

(a) (b)

Fig. 16. SEM images showing the surface morphology of samples Al when using unshaped (a) and shape 2 (b) laser pulses

7. Conclusion

We conclude that by optimization of the temporal shaping of the pulses besides the other laser parameters (wavelength, energy, beam homogeneity, fluence), one could choose an appropriate regime to eliminate excessive photo-thermal and photomechanical effects and obtain films with desired crystalline phase, number and dimension of grains/particulates, or controlled porosity.

8. Acknowledgment

Part of the experiments were carried out at the Ultraviolet Laser Facility operating at IESL-FORTH and supported by the EU through the Research Infrastructures activity of FP6 (Project: Laserlab-Europe; Contract No: RII3-CT-2003-506350). The authors are thankful to C. Ghica for the electron microscopy analyses. The financial support of the CNCSIS – UEFISCDI, project number PNII – IDEI 1289/2008 is acknowledged.

9. References

Ackermann, R., Salmon, E., Lascoux, N., Kasparian, J., Rohwetter, P., Stelmaszczyk, K., Li, S., Lindinger, A., Woste, L., Bejot, P., Bonacina, L., Wolf, J.-P. (2006) Optimal control of filamentation in air *Applied Physics Letters* volume 89, no. 17 (October 2006) pp. 171117_1-3, ISSN 1077-3118

Amoruso, S., Bruzzese, R., Vitiello, M., Nedialkov, N.N., Atanasov, P.A. (2005a) Experimental and theoretical investigations of femtosecond laser ablation of aluminum in vacuum *Journal of Applied Physics* volume 98, no. 4 (August 2005) pp 044907_1-7, ISSN 1089-7550

Amoruso, S., Ausanio, G., Bruzzese, R., Vitiello, M., Wang, X., (2005b) Femtosecond laser pulse irradiation of solid targets as a general route to nanoparticle formation in a vacuum *Physical Review B* volume 71, no. 3 (January 2005) pp 033406_1-4, ISSN 1550-235X

Amoruso, S., Bruzzese, R., Wang, X., Nedialkov, N.N., Atanasov, P.A. (2007) An analysis of the dependence on photon energy of the process of nanoparticle generation by femtosecond laser ablation in a vacuum *Nanotechnology* volume 18, no. 14 (April 2007) pp 145612, ISSN 1361-6528

Assion, A., Baumert, T., Bergt, M., Brixner, T., Kiefer, B., Seyfried, V., Strehle, M., Gerber, G., (1998) Control of chemical reactions by feedback-optimized phase-shaped femtosecond laser pulses *Science* volume 282, no. #5390 (October 1998) pp 919-922, ISSN 1095-9203

Assion, A., Wollenhaupt, M., Haag, L., Mayorov, F., Sarpe-Tudoran, C., Winter, M., Kutschera, U., Baumert, T. (2003) Femtosecond laser-induced-breakdown spectrometry for Ca^{2+} analysis of biological samples with high spatial resolution *Applied Physics B; Lasers and Optics* volume 77, no. 3 (2003) pp 391-397, ISSN 1432-0649

Banks, P.S., Dinh, L., Stuart, B.C., Feit, M.D., Komashko, A.M., Rubenchik, A.M., Perry, M.D., McLean, W. (1999) Short-pulse laser deposition of diamond-like carbon thin films *Applied Physics A: Materials Science & Processing* volume 69, supplement 1 (December 1999) pp S347–S353, ISSN 1432-0630

Barcikowski, S., Hahn, A., Kabashin, A.V., Chichkov, B.N. (2007) Properties of nanoparticles generated during femtosecond laser machining in air and water *Applied Physics A: Materials Science & Processing* volume 87, no. 1 (April 2007) pp 47-55, ISSN 1432-0630

Bartels, R., Backus, S., Zeek, E., Misoguti, L., Vdovin, G., Christov, I. P., Murnane, M. M., Kapteyn, H. C. (2000) Shaped-pulse optimization of coherent emission of high-harmonic soft X-rays *Nature* volume 406, no. 6792 (July 2000) pp 164-166, ISSN 0028-0836

Belouet, C. (1996) Thin film growth by the pulsed laser assisted deposition technique *Applied Surface Science* volume 96-98 (April 1996) pp 630-642, ISSN 0169-4332

Brown, D.M., Downey, E. Grezzo, M. Kretchmer, J. Krishnamethy, V. Hennessy, W. Michon, G. (1996) Silicon carbide MOSFET technology *Solid State Electronics* volume 39, no. 11 (November 1996) pp 1531- 1542, ISSN 0038-1101

Bulgakova, N.M., Stoian, R., Rosenfeld, A., Hertel, I.V. (2010) Continuum models of ultrashort pulsed laser ablation in *Laser-Surface Interactions for New Materials Production Tailoring Structure and Properties*, Miotello, Antonio; Ossi, Paolo M. (Eds.) pp 81-97, Springer Series in Materials Science, Vol. 130, ISBN 978-3-642-03306-3, Springer Heidelberg Dordrecht London New York

Cheung, J.T. (1994) History and Fundamentals of Pulsed Laser Deposition in *Pulsed Laser Deposition of Thin Films,* Chrisey, D. B., Hubler G. K. (Eds.) pp 1-22, John Wiley &Sons, Inc., ISBN 0471592188 9780471592181, New York

Chichkov, B., Momma, N. C., Nolte, S., von Alvensleben, F., Tunnermann, A. (1996) Femtosecond, picosecond and nanosecond laser ablation of solids *Applied Physics A: Materials Science & Processing* volume 63, no. 2 (July 1996) pp 109-115; ISSN 1432-0630

Chrisey, D. B., Hubler G. K. (Eds.) (1994) *Pulsed Laser Deposition of Thin Films* J. Wiley, ISBN 0471592188 9780471592181, New York

Claeyssens, F., Ashfold, M.N.R., Sofoulakis, E., Ristoscu, C.G., Anglos, D., Fotakis, C. (2002) Plume emissions accompanying 248 nm laser ablation of graphite in vacuum: Effects of pulse duration *Journal of Applied Physics* volume 91, no. 9 (May 2002) pp 6162-6172, ISSN 1089-7550

Colombier, J.P., Combis, P., Rosenfeld, A., Hertel, I.V., Audouard, E., Stoian, R. (2006) Optimized energy coupling at ultrafast laser-irradiated metal surfaces by tailoring intensity envelopes: Consequences for material removal from Al samples *Physical Review B* volume 74, no. 22 (December 2006) pp 224106_1-16, ISSN 1550-235X

Dachraoui, H., Husinsky, W. (2006) Thresholds of Plasma Formation in Silicon Identified by Optimizing the Ablation Laser Pulse Form *Physical Review Letters* volume 97, no. 10 (September 2006) pp 107601_1-4, ISSN 1079-7114

Dausinger, F., Lichtner, F., Lubatschowski, H. (Eds.) (2004) *Femtosecond Technology for Technical and Medical Applications,* Topics in Applied Physics, Vol. 96, Springer, ISBN 3-540-20114-9 Springer Berlin Heidelberg New York

DeLong, K.W.; Trebino, R.; Hunter, J.; White, W.E. (1994) Frequency-resolved optical gating with the use of second-harmonic generation *Journal of the Optical Society of America B* volume 11, no. 11 (November 1994) pp 2206-2215, ISSN 1520-8540

Eliezer, S., Eliaz, N., Grossman, E., Fisher, D., Gouzman, I., Henis, Z., Pecker, S., Horovitz, Y., Fraenkel, M., Maman, S., Lereah, Y. (2004) Synthesis of nanoparticles with

femtosecond laser pulses *Physical Review B* volume 69, no. 14 (April 2004) pp 144119_1-6, ISSN 1550-235X

Englert, L., Rethfeld, B., Haag, L., Wollenhaupt, M., Sarpe-Tudoran, C., Baumert, T. (2007) Control of ionization processes in high band gap materials via tailored femtosecond pulses *Optics Express* volume 15, no. 26 (December 2007) pp 17855-17862, ISSN 1094-4087

Englert, L., Wollenhaupt, M., Haag, L., Sarpe-Turdoran, C., Rethfeld, B., Baumert, T. (2008) Material processing of dielectrics with temporally asymmetric shaped femtosecond laser pulses on the nanometer scale *Applied Physics A: Materials Science & Processing* volume 92, no. 4 (September 2008) pp 749-753, ISSN 1432-0630

Gamaly, E.G., Rode, A.V., Uteza, O., Kolev, A., Luther-Davies, B., Bauer, T., Koch, J., Korte, F., Chichkov, B.N. (2004) Control over a phase state of the laser plume ablated by femtosecond laser: Spatial pulse shaping *Journal of Applied Physics* volume 95, no. 5 (March 2004) pp 2250-2257, ISSN 1089-7550

Gamaly, E.G., Rode, A.V., Luther-Davies, B. (2007) Ultrafast laser ablation and film deposition in *Pulsed laser deposition of thin films: Applications-led growth of functional materials*, Edited by Robert Eason, pp 99-129, John Willey & Sons, Inc., ISBN-13: 978-0-471-44709-2, Hoboken, New Jersey

Garrelie, F., Loir, A.S., Donnet, C., Rogemond, F., Le Harzic, R., Belin, M., Audouard, E., Laporte, P. (2003) Femtosecond pulsed laser deposition of diamond-like carbon thin films for tribological applications *Surface and Coatings Technology* volume 163–164 (January 2003) pp 306-312, ISSN 0257-8972

Geretovszky, S., Kantor, Z., Szorenyi, T. (2003) Structure and composition of carbon-nitride films grown by sub-ps PLD *Applied Surface Science* volume 208–209 (March 2003) pp 547-552; ISSN 0169-4332

Ghica, C., Ristoscu, C., Socol, G., Brodoceanu, D., Nistor, L.C., Mihailescu, I.N., Klini, A., Fotakis, C. (2006) Growth and characterization of β-SiC films obtained by fs laser ablation *Applied Surface Science* volume 252, no. 13 (April 2006) pp 4672–4677, ISSN 0169-4332

Golan, B., Fradkin, Z., Kopnov, G., Oron, D., Naaman R. (2009) Controlling two-photon photoemission using polarization pulse shaping *The Journal of Chemical Physics* volume 130 no 6 (February 2009) pp 064705_1-6, ISSN 1089-7690

Grojo, D., Hermann, J., Perrone, A. (2005) Plasma analyses during femtosecond laser ablation of Ti, Zr, and Hf *Journal of Applied Physics* volume 97, no. 6 (March 2005) pp 063306_1-9, ISSN 1089-7550

Guillermin, M., Liebig, C., Garrelie, F., Stoian, R., Loir, A.-S., Audouard, E. (2009) Adaptive control of femtosecond laser ablation plasma emission *Applied Surface Science* volume 255, no. 10 (March 2009) pp 5163–5166, ISSN 0169-4332

Gunaratne, T., Kangas, M., Singh, S., Gross, A., Dantus, M. (2006) Influence of bandwidth and phase shaping on laser induced breakdown spectroscopy with ultrashort laser pulses *Chemical Physics Letters* Volume 423, no. 1-3 (May 2006) pp 197-201, ISSN 0009-2614

Gyorgy, E., Ristoscu, C., Mihailescu, I.N., Klini, A., Vainos, N., Fotakis, C., Ghica, C., Schmerber, G., Faerber, J. (2001) Role of laser pulse duration and gas pressure in deposition of AlN thin films *Journal of Applied Physics*, volume 90, no. 1 (July 2001) pp 456-461, ISSN 1089-7550

Gyorgy, E., Teodorescu, V.S., Mihailescu, I.N., Klini, A., Zorba, V., Manousaki, A., Fotakis, C. (2004) Surface Morphology Studies of Sub-Ps Pulsed-Laser-Deposited AlN Thin Film *Journal of Materials Research* volume 19, no. 3 (March 2004) pp 820-826, ISSN 2044-5326

Hergenroder, R., Miclea, M., Hommes, V., (2006) Controlling semiconductor nanoparticle size distributions with tailored ultrashort pulses *Nanotechnology* volume 17, no. 16 (August 2006) pp 4065-4071, ISSN 1361-6528

http://www.nasatech.com/Briefs/Feb04/LEW17186.html

Hu, Z., Singha, S., Liu, Y., Gordon, R.J. (2007) Mechanism for the ablation of Si(111) with pairs of ultrashort laser pulses *Applied Physics Letters* volume 90, no. 13 (March 2007) pp 131910_1-3, ISSN 1077-3118

Itina, T. E., Shcheblanov, N. (2010) Electronic excitation in femtosecond laser interactions with wide-band-gap materials *Applied Physics A: Materials Science & Processing* volume 98, no. 4 (March 2010) pp 769–775, ISSN 1432-0630

Jegenyes, N., Toth, Z., Hopp, B., Klebniczki, J., Bor, Z., Fotakis, C. (2006) Femtosecond pulsed laser deposition of diamond-like carbon film: The effect of double laser pulses *Applied Surface Science* volume 252, no. 13 (April 2006) pp 4667-4671, ISSN 0169-4332

Judson, R.S., Rabitz, H. (1992) Teaching lasers to control molecules *Physical Review Letters* volume 68, no. 10 (March 1992) pp 1500-1503, ISSN 1079-7114

Kaganov, M. I., Lifshitz, I. M., Tanatarov, L. V. (1957) Relaxation between electrons and the crystalline lattice *Soviet Physics – JETP* volume 4 (1957) pp 173-180, ISSN 0038-5646

Klini, A., Loukakos, P.A., Gray, D., Manousaki, A., Fotakis, C. (2008) Laser Induced Forward Transfer of metals by temporally shaped femtosecond laser pulses *Optics Express* Vol. 16, No. 15 (July 2008) pp 11300-11309, ISSN 1094-4087

Lozovoy, V.V., Xu, B., Coello, Y., Dantus, M. (2008) Theoretical development of a high-resolution differential-interference-contrast optic for x-ray microscopy *Optics Express* volume 16, no. 2 (January 2008) pp 592-597, ISSN 1094-4087

Luculescu, C.R., Miyake, H., Sato, S. (2002) Deposition of BN thin films onto Si(1 0 0) substrate by PLD with nanosecond and femtosecond pulses in nitrogen gas background *Applied Surface Science* volume 197–198 (September 2002) pp 499–504, ISSN 0169-4332

Mihailescu, I.N., Hermann, J. (2010) Laser Plasma Interactions *Laser Processing of Materials: Fundamentals, Applications, and Developments*, Ed. P. Schaaf, pp 51–90, Springer Series in Materials Science, ISBN 978-3-642-13280-3, Springer Heidelberg Dordrecht London New York

Miller, J.C. (Ed.) (1994) *Laser Ablation Principles and Applications*, Springer-Verlag, ISBN 3540575715 9783540575719 Berlin

Miller, J. C., Haglund, R.F. (Eds.) (1998) *Laser Ablation and Desorption*, Academic Press, ISBN 0124759750 9780124759756, San Diego

Millon, E., Albert, O., Loulergue, J. C., Etchepare, J. C., Hullin, D., Seiler, W., Perriere, J. (2000) Growth of heteroepitaxial ZnO thin films by femtosecond pulsed-laser deposition *Journal of Applied Physics* volume 88, no. 11 (December 2000) pp 6937-6939; ISSN 1089-7550

Muller, G., Krotz, G., Niemann, E. (1994) SiC for sensors and high-temperature electronics *Sensors and Actuators A: Physical* volume 43, no. 1-3 (May 1994) pp 259-268, ISSN 0924-4247

Okoshi, M., Higashikawa, K., Hanabusa, M. (2000) Pulsed laser deposition of ZnO thin films using a femtosecond laser *Applied Surface Science* volume 154–155 (February 2000) pp 424-427, ISSN 0169-4332

Palmour, J. W., Edmond, J.A., Kong, H. S., Carter Jr., C.H. (1993) 6H-silicon carbide devices and applications *Physica B: Condensed Matter* volume 185, no 1-4 (April 1993) pp 461-465, ISSN 0921-4526

Papastathopoulos, E., Strehle, M., Gerber, G. (2005) Optimal control of femtosecond multiphoton double ionization of atomic calcium *Chemical Physics Letters* volume 408, no. 1-3 (June 2005) pp 65-70, ISSN 0009-2614

Parker, D.S.N., Nunn, A.D.G., Minns, R.S., Fielding, H.H. (2009) Frequency doubling and Fourier domain shaping the output of a femtosecond optical parametric amplifier: easy access to tuneable femtosecond pulse shapes in the deep ultraviolet *Applied Physics B: Lasers and Optics* volume 94, no. 2 (February 2009) pp 181–186, ISSN 1432-0649

Perriere, J., Millon, E. Seiler, W. Boulmer-Leborgne, C. Craciun, V. Albert, O. Loulergue, J.C. Etchepare, J. (2002) Comparison between ZnO films grown by femtosecond and nanosecond laser ablation *Journal of Applied Physics* volume 91, no. 2 (January 2002) pp 690 - 696, ISSN 1089-7550

Piñon, V., Fotakis, C., Nicolas, G., Anglos, D. (2008) Double pulse laser-induced breakdown spectroscopy with femtosecond laser pulses *Spectrochimica Acta Part B: Atomic Spectroscopy* volume 63, no. 10 (October 2008) pp 1006-1010; ISSN 0584-8547

Pronko, P.P., Cutta, S.K., Squier, J., Rudd, J.V., Du, D., Mourou, G. (1995) Machining of sub-micron holes using a femtosecond laser at 800 nm *Optics Communications* volume 114, no. 1-2 (January 1995) pp 106–110, ISSN 0030-4018

Pronko, P.P., Zhang, Z., Van Rompay, P.A. (2003) Critical density effects in femtosecond ablation plasmas and consequences for high intensity pulsed laser deposition *Applied Surface Science* volume 208–209 (March 2003) pp 492-501, ISSN 0169-4332

Qian, F., Craciun, V., Singh, R.K., Dutta, S.D., Pronko, P.P. (1999) High intensity femtosecond laser deposition of diamond-like carbon thin films *Journal of Applied Physics* volume 86, no. 4 (August 1999) pp 2281-2290, ISSN 1089-7550

Ristoscu, C., Mihailescu, I.N., Velegrakis, M., Massaouti, M., Klini, A., Fotakis, C. (2003) Optical Emission Spectroscopy and Time-of-Flight investigations of plasmas generated from AlN targets in cases of Pulsed Laser Deposition with sub-ps and ns Ultra Violet laser pulses *Journal of Applied Physics* volume 93, no. 5 (March 2003) pp 2244-2250, ISSN 1089-7550

Ristoscu, C. Gyorgy, E. Mihailescu, I. N. Klini, A. Zorba, V. Fotakis, C. (2004) Effects of pulse laser duration and ambient nitrogen pressure in PLD of AlN *Applied Physics A: Materials Science & Processing* volume 79, no 4-6 (September 2004) 927-929 ISSN 1432-0630

Ristoscu, C., Socol, G., Ghica, C., Mihailescu, I.N., Gray, D., Klini, A., Manousaki, A., Anglos, D., Fotakis, C. (2006) Femtosecond pulse shaping for phase and morphology control in PLD: Synthesis of cubic SiC *Applied Surface Science* volume 252, no 13 (April 2006) pp 4857-4862, ISSN 0169-4332

Schmidt, B., Hacker, M., Stobrawa, G., Feurer, T. (n.d.) *LAB2-A virtual femtosecond laser lab* Available from http://www.lab2.de

Sheng, S., Spencer, M.G., Tang, X., Zhou, P., Wongchoitgul, W., Taylor, C., Harris, G. L. (1997) An investigation of 3C-SiC photoconductive power switching devices *Materials Science and Engineering B* volume 46, no. 1-3 (April 1997) pp 147–151, ISSN 0921-5107

Singha, S., Hu, Z., Gordon, R.J. (2008) Ablation and plasma emission produced by dual femtosecond laser pulses *Journal of Applied Physics* volume 104, no. 11 (December 2008) pp 113520_1-10, ISSN 1089-7550

Stoian, R., Boyle, M., Thoss, A., Rosenfeld, A., Korn, G., Hertel, I. V., Campbell, E. E. B. (2002) Laser ablation of dielectrics with temporally shaped femtosecond pulses *Applied Physics Letters* volume 80, no. 3 (January 2002) pp 353-355, ISSN 1077-3118

Stoian, R., Boyle, M., Thoss, A., Rosenfeld, A., Korn, G., Hertel, I. V. (2003) Dynamic temporal pulse shaping in advanced ultrafast laser material processing *Applied Physics A: Materials Science & Processing* volume 77, no. 2 (July 2003) pp 265-269, ISSN 1432-0630

Tanabe, T., Kannari, F., Korte, F., Koch, J., Chichkov, B. (2005) Influence of spatiotemporal coupling induced by an ultrashort laser pulse shaper on a focused beam profile *Applied Optics* volume 44, no. 6 (February 2005) pp 1092-1098, ISSN 2155-3165

Teghil, R., D'Alessio, L., Santagata, A., Zaccagnino, M., Ferro, D., Sordelet, D.J. (2003) Picosecond and femtosecond pulsed laser ablation and deposition of quasicrystals *Applied Surface Science* volume 210, no. 3-4 (April 2003) pp 307-317, ISSN 0169-4332

Trebino, R., Kane, D.J. (1993) Using phase retrieval to measure the intensity and phase of ultrashort pulses: frequency-resolved optical gating *Journal of the Optical Society of America A* volume 10, no. 5 (May 1993) pp 1101–1111, ISSN 1520-8532

Trebino, R., DeLong, K.W., Fittinghoff, D.N., Sweetser, J.N., Krumbügel, M.A., Richman, B.A., Kane, D.J. (1997) Measuring ultrashort laser pulses in the time-frequency domain using frequency-resolved optical gating *Review of Scientific Instruments* volume 68, no. 9 (September 1997) pp 3277-3295, ISSN 1089-7623

Trebino, R. (2002) *Frequency-Resolved Optical Gating: The Measurement of Ultrashort Laser Pulses* Kluwer Academic ISBN 1402070667 9781402070662, Boston

Verluise, F., Laude, V., Cheng, Z., Spielmann, C.H., Tournois, P. (2000) Amplitude and phase control of ultrashort pulses by use of an acousto-optic programmable dispersive filter: pulse compression and shaping *Optics Letters* volume 25, no. 8 (April 2000) pp 575-577, ISSN 1539-4794

Von Allmen, M., Blatter, A. (1995) *Laser-Beam Interactions with Materials* (2nd edition) Springer, ISBN 3540594019 9783540594017, Berlin; Heidelberg; New York; Barcelona; Budapest; Hong Kong; London; Milan; Paris; Tokyo

Wefers, M.M., Nelson, K.A. (1995) Analysis of programmable ultrashort waveform generation using liquid crystal spatial light modulators *Journal of the Optical Society of America B* volume 12, no. 7 (July 1995) pp 1343-1362, ISSN 1520-8540

Weiner, A. M. (2000) Femtosecond pulse shaping using spatial light modulators *Review of Scientific Instruments* volume 71, no. 5 (May 2000) pp 1929-1960, ISSN 1089-7623

Zhang, Z., VanRompay, P.A., Nees, J.A., Clarke, R., Pan, X., Pronko, P.P. (2000) Nitride film deposition by femtosecond and nanosecond laser ablation in low-pressure nitrogen

discharge gas *Applied Surface Science* volume 154–155 (February 2000) pp 165–171, ISSN 0169-4332

Zhigilei, L. V., Garrison, B. J. (2000) Microscopic mechanisms of laser ablation of organic solids in the thermal and stress confinement irradiation regimes *Journal of Applied Physics* volume 88, no. 3 (2000) pp 1281-1298, ISSN 1089-7550

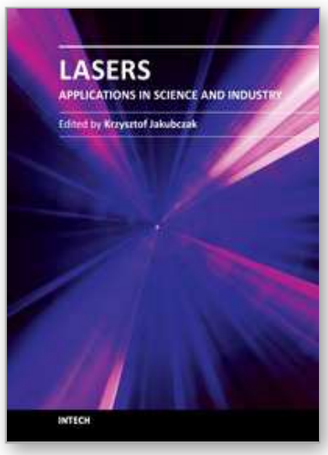

Lasers - Applications in Science and Industry
Edited by Dr Krzysztof Jakubczak

ISBN 978-953-307-755-0
Hard cover, 276 pages
Publisher InTech
Published online 09, December, 2011
Published in print edition December, 2011

The book starts with basic overview of physical phenomena on laser-matter interaction. Then it is followed by presentation of a number of laser applications in the nano-particles and thin films production, materials examination for industry, biological applications (in-vitro fertilization,tissue ablation) and long-range detection issues by LIDARs.

How to reference
In order to correctly reference this scholarly work, feel free to copy and paste the following:

Carmen Ristoscu and Ion N. Mihailescu (2011). Effect of Pulse Laser Duration and Shape on PLD Thin Films Morphology and Structure, Lasers - Applications in Science and Industry, Dr Krzysztof Jakubczak (Ed.), ISBN: 978-953-307-755-0, InTech, Available from: http://www.intechopen.com/books/lasers-applications-in-science-and-industry/effect-of-pulse-laser-duration-and-shape-on-pld-thin-films-morphology-and-structure

INTECH
open science | open minds

InTech Europe
University Campus STeP Ri
Slavka Krautzeka 83/A
51000 Rijeka, Croatia
Phone: +385 (51) 770 447
Fax: +385 (51) 686 166
www.intechopen.com

InTech China
Unit 405, Office Block, Hotel Equatorial Shanghai
No.65, Yan An Road (West), Shanghai, 200040, China
中国上海市延安西路65号上海国际贵都大饭店办公楼405单元
Phone: +86-21-62489820
Fax: +86-21-62489821

IntechOpen